Positron study of microstructure and phase transition in the Fe-doped $YBa_2Cu_{3-x}Fe_xO_y$ system

Zhang Jincang,[1,3] Liu Lihua,[2,3,*] Dong Cheng,[2] Li Jianqi,[2] Chen Hong,[2] Li Xigui,[3] and Cheng Guosheng[3]
[1]*Department of Physics, Shanghai University, Shanghai 200436, China*
[2]*National Laboratory for Superconductivity, Institute of Physics, Chinese Academy of Science, P.O. Box 603, Beijing, 100080, China*
[3]*Department of Physics, Henan Normal University, Xinxiang, 453002, China*
(Received 27 November 2000; revised manuscript received 7 May 2001; published 9 January 2002)

A series of $YBa_2Cu_{3-x}Fe_xO_y$ ($x=0-0.50$) samples has been studied by means of positron annihilation technology, scan electron microscope and x-ray diffraction. The oxygen contents of the samples have been measured using a volumetric method. The positron short-lifetime component τ_1 decreases abruptly between $x=0.12$ and 0.15 where the compound undergoes an *O-T* phase transition and the tweed microstructure disappears. We proposed a simple model to describe the dependency of τ_1 on oxygen vacancy and twin (and tweed) boundary densities. The experimental results can be satisfactorily explained using this model. The positron lifetime τ_1 depends not only on the oxygen vacancy density, but also on the twin and tweed densities. Therefore, the positron can be used as a sensitive probe for the *O-T* phase transition in this system. In addition, analysis of the experimental results also gives certain indication for Fe clustering when $x \geqslant 0.20$.

DOI: 10.1103/PhysRevB.65.054513 PACS number(s): 78.70.Bj, 74.72.Bk, 91.60.Ed

I. INTRODUCTION

Extensive studies have been made on pure and doped $YBa_2Cu_{3-x}Fe_xO_y$ (YBCO) systems and the replacement of Cu by other metals may provide information about the superconducting mechanism.[1,2] In undoped $YBa_2Cu_3O_7$, there are two structurally different Cu sites: Cu(1) and Cu(2). The Cu atoms at the Cu(1) sites have a square planar oxygen coordination and form Cu-O chains; the remaining Cu atoms at the Cu(2) sites have a fivefold pyramidal coordination of oxygen and form the CuO_2 plane. The oxygen atoms in the Cu-O chain are not strongly bound and can be removed easily from the lattice. Usually, YBCO is oxygen deficient with oxygen vacancies mainly located in the Cu-O chain.

Previous studies of Fe-YBCO were conducted by many experimental methods including thermogravimetric analysis, powder x-ray diffraction, neutron powder diffraction, Mössbauer spectroscopy, transition electron microscopy, etc.[1–5] The main conclusions concerning its crystal structure and microstructure are the following.

(I) The Fe atoms locate primarily at the Cu(1) sites at the low doping level; upon increasing the Fe concentration, some of the Cu(2) sites become occupied.

(II) During the replacement of Cu^{2+} by the trivalent ion Fe^{3+}, the oxygen content will increase for the charge compensation. The oxygen content, which influences T_c tremendously, also depends on the processing conditions.

(III) $YBa_2Cu_{3-x}Fe_xO_y$ undergoes a structural phase transition from orthorhombic to tetragonal at a certain Fe doping level.

(IV) The microstructure of $YBa_2Cu_{3-x}Fe_xO_y$ evolves as the Fe content changes. Twin structure predominates when x is low ($x \leqslant 0.02$). With the increasing of x, tweed structure appears and its proportion increases successively until it becomes dominate ($x=0.08$). When $x=0.15$, the tweed structure disappears completely.[5] Detailed dark-field transmission electron micrographs and the electron-diffraction pattern are illustrated in Ref. 5.

Positron annihilation technology (PAT) has been recognized as a very useful and sensitive probe of the electronic structure, the defects at atomic size, and the structural phase transition, and has been successfully used to study these properties in metals, semiconductors and superconductors.[6–8] Von Stetten *et al.*,[9] Jean *et al.*,[10] and Chakraborty *et al.*[11] proved by theory and experiment that the positrons in YBCO mainly probe the Cu-O chain region and are very sensitive to the oxygen vacancy. On the other hand, the twin (and tweed) boundary is also the shallow trap centers for positron annihilation.[6]

Considering the structural properties of the Fe-doped YBCO system and the characteristics of the positron annihilation technology, as we mentioned above, it is important to study the Fe substitute YBCO system by PAT. Zhang conducted a positron annihilation experiment on Fe-doped YBCO and concluded that the positron annihilation short-lifetime component is inversely proportional to the Fe concentration.[12] It should be noted that their samples were prepared in flowing oxygen at a slow-cooling rate. Ishibashi *et al.* studied the thermal effect of positron annihilation in the trapping center: namely, the temperature dependence of lifetime between 20 K and room temperature.[13] In this work, we prepared the $YBa_2Cu_{3-x}Fe_xO_y$ ($x=0-0.5$) specimens in air and studied them using positron annihilation technology. In order to get a reasonable and perfect explanation for our experimental results, we determined the oxygen content and calculated the number of valid oxygen vacancy per unit cell for each specimen. A simple model is proposed to explain the dependence of positron lifetime on the variations of the imperfections in this system. The experimental results show that both the oxygen vacancies and the twin (and tweed) boundaries are the dominant trapping centers for positron. Our experiments also supported our assumption that the positron can be used as a sensitive probe for the orthorhombic-tetragonal phase transition in the YBCO system. In addition, analysis of the experimental results also gives certain indication for Fe clustering when $x \geqslant 0.20$.

II. EXPERIMENTS

Samples of $YBa_2Cu_{3-x}Fe_xO_y$ ($x=0-0.5$) were prepared by solid-state reactions from appropriate amounts of high-purity Y_2O_3, $BaCO_3$, CuO, and Fe_2O_3. The starting materials were thoroughly mixed and calcined first at 900 °C for 24 h in air to get the precursor. Then, the precursors were reground, pressed as tablets, and heated to 900 °C for 24 h followed by cooling down to room temperature at a rate of 20 °C/h. All samples were prepared in identical conditions.

The structures of the samples were analyzed by powder x-ray diffraction using an MXP-AHF18 diffractometer. The temperature dependencies of resistance were measured using standard dc four-probe method with the voltage resolution of 10^{-7} V. Susceptibility data were obtained by the induction method from 4.2 K to room temperature. The electron diffraction and high-resolution electron microscopy (HREM) studies were performed using a H-9000NA electron microscope. Thin specimens were prepared by crushing the samples into fine fragments with CCl_4, which were then dispersed on Cu grids coated with wholly carbon support films.

The positron lifetime spectra were measured at room temperature using an ORTEC-100U fast-fast coincidence lifetime spectrometer with a time resolution of 220 ps as measured with the ^{60}Co radioisotope. Two pieces of identical samples were sandwiched with a $10\mu c_i$ ^{22}Na positron source deposited on a thin Mylar foil. Each spectrum contained more than 1×10^6 counts. After subtracting background and source contributions, the lifetime spectra were analyzed in two-lifetime components by the POSITRONFIT-EXTENDED program with the best fit $\chi^2\leqslant1.2$.

The oxygen content of the samples was determined by a volumetric method. The experimental detail for oxygen content determination will be discussed elsewhere. Therefore, we only present the principle of the method here. Dissolving sample in diluted hydrochloric acid, the following chemical reaction will take place:

$$\begin{aligned} &YBa_2Cu_{3-x}Fe_xO_y+(13+x)HCl \\ &\quad=YCl_3+2BaCl_2+(3-x)CuCl_2 \\ &\qquad+xFeCl_3+(13+x)/2H_2O \\ &\qquad+[y-(13+x)/2]2O_2. \end{aligned} \tag{1}$$

According to Eq. (1), we have

$$\frac{M}{F}=\frac{m}{[y-0.5(13+x)]\times16}. \tag{2}$$

where M and F are the mass and molecular weight of the sample, respectively. m is the mass of the oxygen liberated in the above reaction. x refers to the doping content in $YBa_2Cu_{3-x}Fe_xO_y$. Therefore, the oxygen content y can be obtained using Eq. (2).

III. RESULTS AND DISCUSSION

A. Crystal structure, oxygen content, and T_c

The x-ray-diffraction patterns for some typical specimens are shown in Fig. 1. In all diffraction patterns, no observable impurity peak is found. The lattice parameters of the samples were calculated by the least-squares method using the POWDERX program[14] and the results are listed in Table I. The substitution of Cu with Fe induces an *O-T* structure phase transition. Within the orthorhombic range the lattice parameter a increases and b decreases as x increases. When $x=0.15$, the structural phase transition is completed and the lattice parameters a and b become identical.

The zero resistance temperature T_c and oxygen content y for each specimen are also listed in Table I. The dependence of T_c on Fe content is consistent with the reported results (Ref. 1). The slight discrepancy is attributed to the different preparation conditions. T_c decreases continuously with increasing Fe content and is less than 4.2 K at $x=0.3$. Further Fe doping results in semiconducting behavior, i.e., resistance increasing with decreasing temperature. The tetragonal phases where $x=0.15$, 0.2, and 0.25 show superconducting transition at 55.5, 48, and 40 K, respectively. The resistance variations of some samples, from room temperature to 4.2 K, is shown in Fig. 2. All samples with x less than 0.15 show metallic behavior above T_c, while the resistance of samples with $x=0.20$ and 0.25 increase as the temperature decreases from 150 K to the onset of the superconducting transition. The superconducting transition width increases with the substituted Fe content.

The oxygen content was determined at least 3 times for each specimen, and the average values (y_{exp}) are listed in the Table I. The uncertainty of the volume determination was less than $\pm0.5\%$. The oxygen content is nearly a constant at low doping levels, and it increases with increasing Fe concentration when x is greater than 0.2. The value of x at which the oxygen content starts to increase does not seem to correlate with the onset of the *O-T* structure transition.

B. Transmission electron microscopy

In order to study the effect of the phase transition on microstructure in detail, a transmission electron microscopy study was performed. Figure 3 shows the zero-axis electron diffraction pattern and the respective dark-field transmission electron micrographs for specimens with $x=0.08$, 0.12, and 0.15. As we can see from Fig. 3, the twins are absent in the transmission electron micrograph image and a very fine tweed structure is evident when $x=0.08$ and 0.12. Associated with the tweed structure are the diffuse streaks at the diffracted spots along the [110] and $[\bar{1}10]$ directions. The dimension of the square microdomain in $x=0.12$ sample is smaller than that of the $x=0.08$ sample and the twin (tweed) boundary density increases as x increases. However, for sample $x=0.15$, the tweed structure in the image and the diffuse streaks at the diffracted spots, which can be seen when $x<0.15$, disappear simultaneously. As a result, the tweed boundary density drops abruptly.

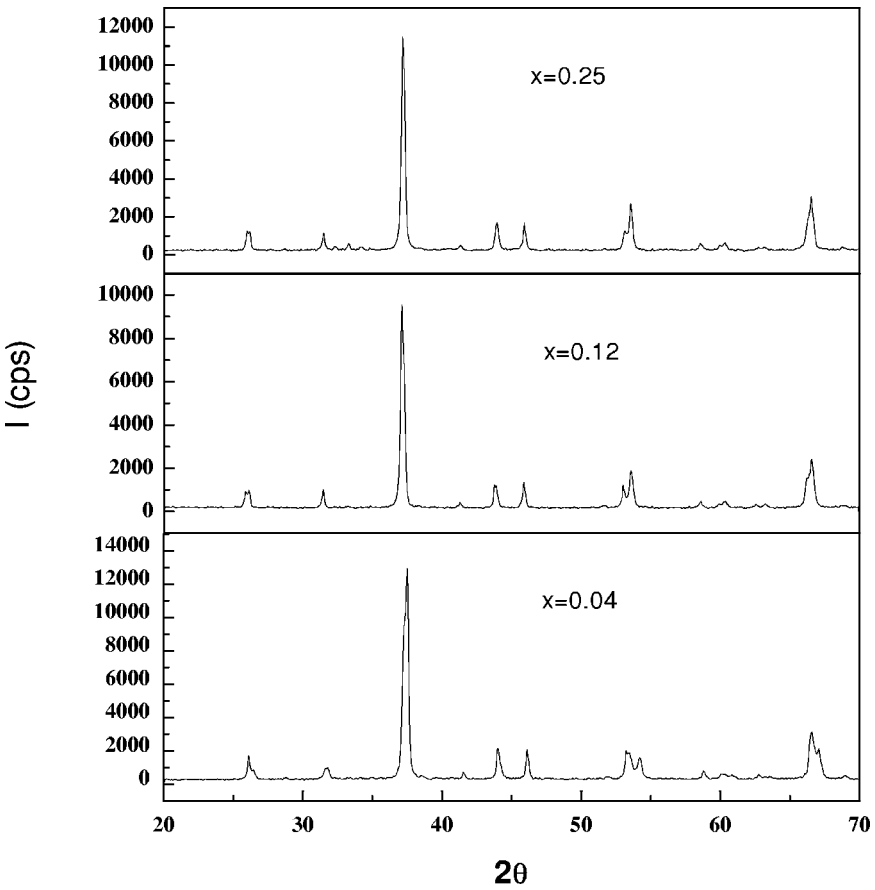

FIG. 1. X-ray-diffraction pattern in the $YBa_2Cu_{3-x}Fe_yO_y$ system. All samples showed no observable impurity peaks in the x-ray-diffraction pattern.

There have been some attempts to interpret the diffuse scattering and the tweedlike morphology in these systems. A previous study of $YBa_2Cu_{3-x}Fe_xO_y$ by high-resolution electron microscopy led Hiroi *et al.* to conclude that the tweed structure and the streaks are due to microdomains of the orthorhombic phase. They also suggested that the domains are squares and each corner of the square domain is occupied by Fe atoms.[15] Considering the different valences and coordination number of Cu^{2+} and Fe^{3+}, we can describe the formation mechanism of the tweed microstructure as follows. Copper atoms located in the Cu-O chains have only fourfold coordination. If we substitute Fe^{3+} for Cu^{2+}, these Fe^{3+} impurities tend to attract more oxygen atoms than Cu^{2+} in order to keep charge balance. Therefore, either copper loses a nearest-neighbor oxygen or extra oxygen atoms have to be put into the Cu-O plane. Because most oxygen positions along the Cu-O chain (*b* direction) are occupied, the extra oxygen atoms will be placed along the a direction. This leads to the formation of new Cu-O chains perpendicular to the original ones. In other words, the random occupa-

TABLE I. Lattice parameters, experimental and calculated oxygen contents, zero-resistance temperature T_c, positron lifetimes, and their intensities of $YBa_2Cu_{3-x}Fe_xO_y$.

x	a (Å)	b (Å)	c (Å)	y_{expt}	y_{cal}	Δ	T_c (K)	τ_1 (ps)	I_1 (%)	τ_2 (ps)	I_2 (%)
0.00	3.8201	3.8879	11.6787	6.98	7.00	0.02	91	187	87.21	525	12.79
0.02	3.8228	3.8882	11.6730	6.97	7.01	0.04	90	192	86.31	534	13.69
0.04	3.8386	3.8811	11.7012	6.97	7.02	0.05	84	193	84.87	521	15.13
0.08	3.8524	3.8700	11.7003	6.95	7.04	0.09	81	196	86.94	526	13.06
0.10	3.8535	3.8672	11.7001	6.965	7.05	0.085	75	200	85.44	523	14.56
0.12	3.8597	3.8658	11.6955	6.964	7.06	0.096	68	201	86.93	543	13.07
0.15	3.8630	3.8630	11.6938	6.99	7.075	0.085	55.5	194	84.61	495	15.93
0.20	3.8634	3.8634	11.6910	6.99	7.10	0.11	48	198	85.52	501	14.48
0.25	3.8702	3.8702	11.6952	7.04	7.125	0.085	40	200	85.81	495	14.19
0.30	3.8696	3.8696	11.6928	7.05	7.15	0.10		198	84.51	492	15.49
0.40	3.8711	3.8711	11.6825	7.06	7.20	0.14		199	84.99	481	15.01
0.50	3.8754	3.8754	11.6867	7.08	7.25	0.17		197	84.75	493	15.25

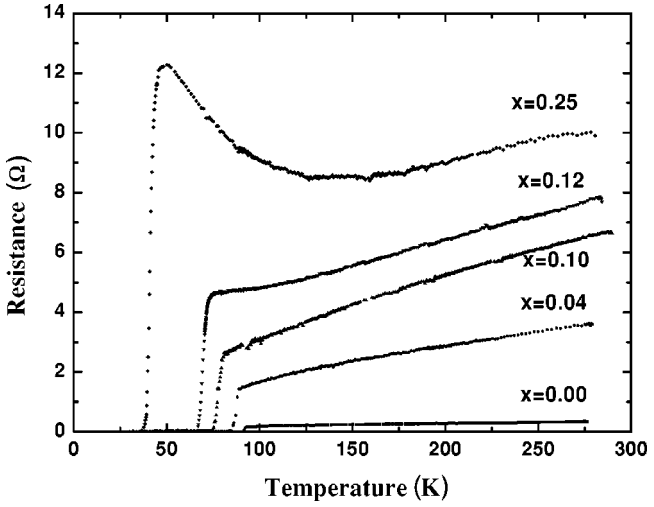

FIG. 2. Resistance vs temperature curve for several $YBa_2Cu_{3-x}Fe_xO_y$ samples from 300 to 4.2 K.

tion of Fe on the Cu(1) site induces the grain boundaries developing along two perpendicular directions and the tweed structure is produced. The selected-area electron diffraction patterns show narrow streaks of diffuse scattering along the [110] and $[\bar{1}10]$ directions through most of the diffracted spots, thus forming a cross.

When $x \geqslant 0.15$, the lattice parameters *a* and *b* become symmetrically equivalent in the tetragonal structure and there are no differences between the [110] and $[\bar{1}10]$ directions any more. Consequently, the tweed structure disappears and the crosses in the diffraction patterns submerge.

C. Positron annihilation experiment

In the YBCO compounds, the positron annihilation processes include free-state annihilation and trapping-state annihilation. The free-state annihilation occurs at the perfect crystal areas and the corresponding positron lifetime is between 160 and 180 ps.[16,17] The trapping-state annihilation refers to the annihilation that take places at the imperfect areas where the electron densities are low. Owing to the Coulomb attraction effect, positrons are trapped easily by defects and annihilated soon after that. The positrons annihilated at the low-electron-density areas have a longer lifetime because positron lifetime varies inversely as the electron density.[18] We divide the trapping-state annihilation areas into shallow trap areas and deep trap areas. The shallow trap areas including oxygen vacancy, twin boundary, dislocation, cation vacancies, etc., where the positron lifetime varies between 200 and 300 ps.[6] Deep trap areas are porosities and cracks, and positron lifetimes are longer than 400 ps.[19]

The variation of the positron short-lifetime component τ_1 as a function of Fe substitution content *x* is plotted in Fig. 4. Here τ_1 increases from 187 to 201 ps as *x* increases from 0.0 to 0.12. Then τ_1 falls sharply to 194 ps at $x=0.15$. When $x>0.15$, τ_1 gradually increases and reaches saturation after $x=0.2$. There is a sudden drop when $x=0.15$ in the curve. If the single datum point is removed, the sharp drop will disappear. We must find some evidence to determine that this

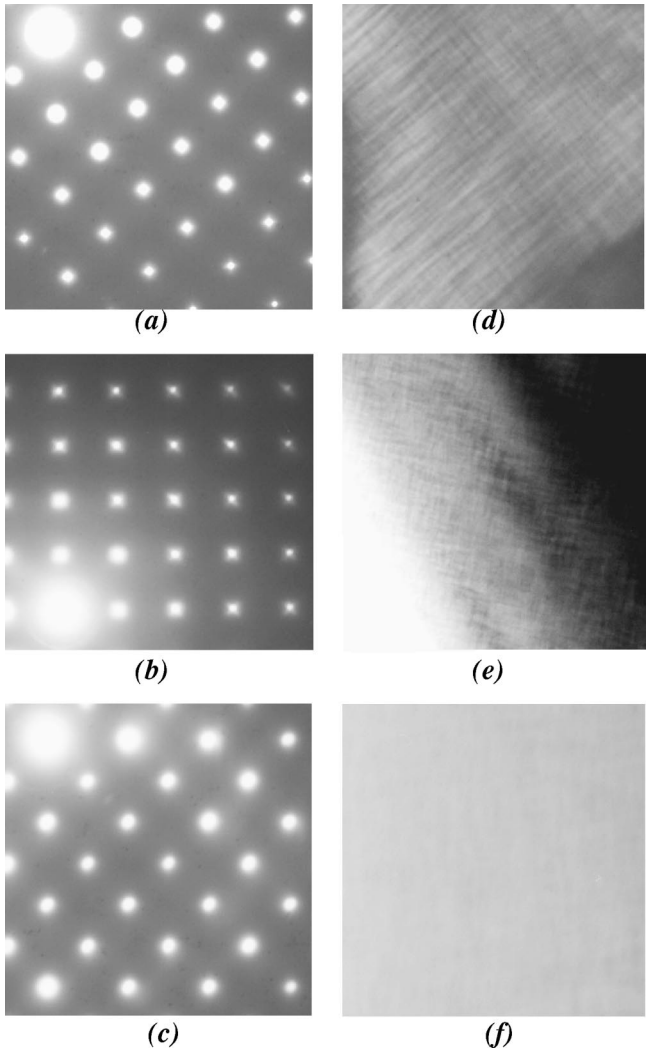

FIG. 3. [001] zone-axis electron diffraction patterns of $YBa_2Cu_{3-x}Fe_xO_y$ are shown in (a) $x=0.08$, (b) $x=0.12$, and (c) $x=0.15$. (d), (e), and (f) are the respective dark-field transmission electron micrographs. Note that the diffuse streaks along both of the [110] and $[\bar{1}10]$ directions at each of the diffracted spots in (a) and (b). When $x=0.15$, the tweed structure in the image and the diffuse streaks at the diffracted spots disappear simultaneously.

sharp drop is not accidental. Therefore, we prepared a series of Co-doped YBCO samples ($YBa_2Cu_{3-x}Co_xO_y$, $x=0.0-0.5$) using identical preparation conditions and studied them using the same experiment technology. We found that Co-doped YBCO samples show the same variation trend of τ_1 as the Fe-doped ones. The positron short-lifetime component τ_1 increases from 187 to 203 ps as *x* increases from 0.0 to 0.12. Then τ_1 also falls sharply to 197 ps at $x=0.15$. Therefore, the sudden drop of τ_1 at $x=0.15$ is intrinsic, and it is not an artifact originating from the difference in the preparation process. According to superimposed-atom calculations, the single oxygen vacancy and twin (tweed) boundary are the weak traps for the positron. Their binding energies are low, and their positron lifetime merely slightly exceeds that of a free state (τ_f).[20] It causes the problem that annihilation in the free state and shallow trapping centers

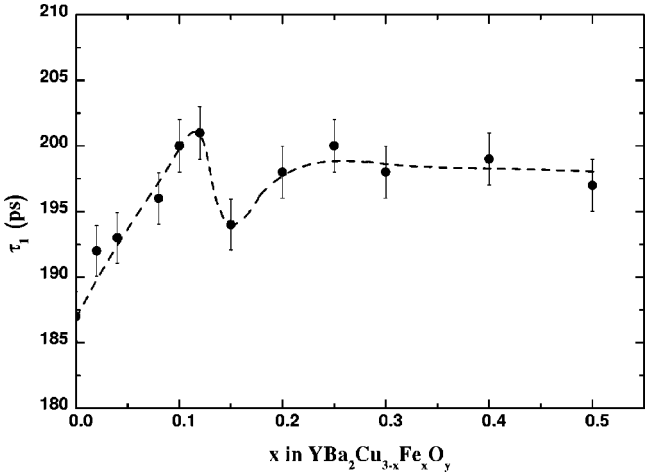

FIG. 4. Positron short-lifetime component τ_1 vs x for $YBa_2Cu_{3-x}Fe_xO_y$, which were obtained from a two-component analysis.

could not be accurately separated. We had attempted a three-lifetime component fit on our spectra, but the results are not reliable. The obtained χ^2 values are very large, and the standard deviations are even larger than the lifetime themselves. This indicates that the lifetime of the shallow trap centers cannot be resolved from the free-state lifetime, in agreement with the theoretical calculation. However, the results of two-lifetime component analyses are reasonable. τ_1 ranges from 187 to 201 ps, which is larger than the free-state lifetime (τ_f) and smaller than the lifetime of the trapping centers such as the oxygen vacancy and twin (tweed) boundary. In such a case, τ_1 is the average positron annihilation time in free and shallow trapping states. The variation of positron long-lifetime component τ_2 as a function of Fe substitution content x is plotted in Fig. 5. Before the phase transition, τ_2 varied between 521 and 543 ps. Then τ_2 has a sharp drop to 495 ps where the *O-T* phase transition occurs and after that τ_2 varied between 501 and 481 ps.

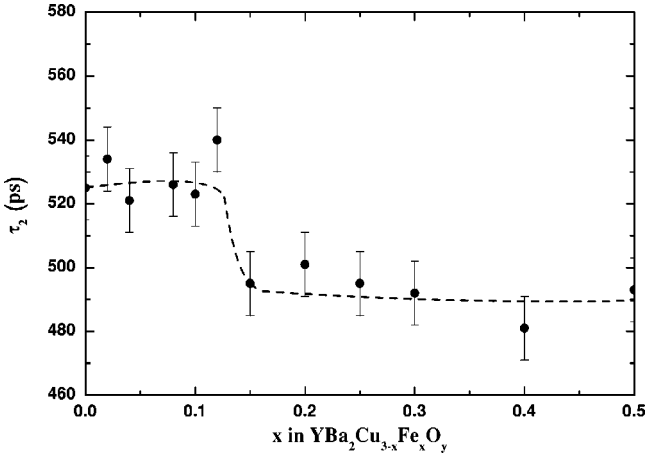

FIG. 5. Positron long-lifetime component τ_2 vs x for $YBa_2Cu_{3-x}Fe_xO_y$, which were obtained from a two-component analysis.

According to the trapping model,[21] the value of the positron characteristic parameter should be the weighted average of their values at the free and trapping states:

$$\tau_1 = P_f \tau_f + P_v \tau_v , \tag{3}$$

$$P_f = \frac{\lambda_f}{\lambda_f + K_v C_v}, \tag{4}$$

$$P_v + P_f = 1, \tag{5}$$

where P_f and P_v are the relative proportion of the positron annihilated at the free and trapping states. τ_f and τ_v are the positron lifetime of the free and trapping states, respectively. λ_f is the annihilation rate of the free state, and K_v is the trapping rate of the trapping center.

Based on the structural characteristics of the Fe-doped YBCO system and our experimental results, we proposed a simple model to describe the relationship between τ_1 and the imperfections in this system. In this model, oxygen vacancies and twin (and tweed) boundaries are two major trapping centers that cause the variation of τ_1. The densities of the other trapping centers do not change significantly with Fe content so that their contribution to τ_1 can be considered as a constant. According to this model, Eq. (3) can be rewritten as

$$\tau_1 = P_f \tau_f + P_{vo} \tau_{vo} + P_{vt} \tau_{vt} \tag{6}$$

where P_{vo} and P_{vt} are the relative proportion of a positron annihilated in the oxygen vacancy and twin (tweed) boundary, respectively, τ_{vo} and τ_{vt} are their corresponding lifetimes. The proportion of the positron annihilated in the free state and shallow trapping center varied between 84.5% and 87.2% in our experiment (see Table I) and can be considered as a constant, so we have

$$P_f = \frac{\lambda_f}{\lambda_f + K_{vo} C_{vo} + K_{vt} C_{vt}}, \tag{7}$$

$$P_{vo} + P_{vt} = 1 - P_f . \tag{8}$$

For certain defections such as the oxygen vacancy and twin (tweed) boundary, their formation energy, size and binding energy are all definite under a particular temperature. The positron annihilation experiments were conducted at room temperature, so the lifetimes of the positron annihilated in an oxygen vacancy (τ_{vo}) and twin (tweed) boundary (τ_{vt}) can be considered definite in every sample. We assume that τ_f, τ_v, and K_v are all positive constants. Therefore, τ_1 is only dependent on C_v, the concentration of trapping centers. It is clearly that when C_{vo} and C_{vt} increase, P_f will decrease and $P_{vo} + P_{vt}$ increase. In other words, if the concentrations of oxygen vacancy and twin (tweed) boundary increase, the relative proportion of the positron annihilated in the shallow trapping centers will also increase, which made τ_1 increase because τ_{v1} and τ_{v2} are both larger than τ_f.

In order to understand the dependence of τ_1 on the doping content, it is necessary to know the variation trend of oxygen vacancies and twin (and tweed) boundary. We consider the formation of oxygen vacancies at first. The substitute Fe ions

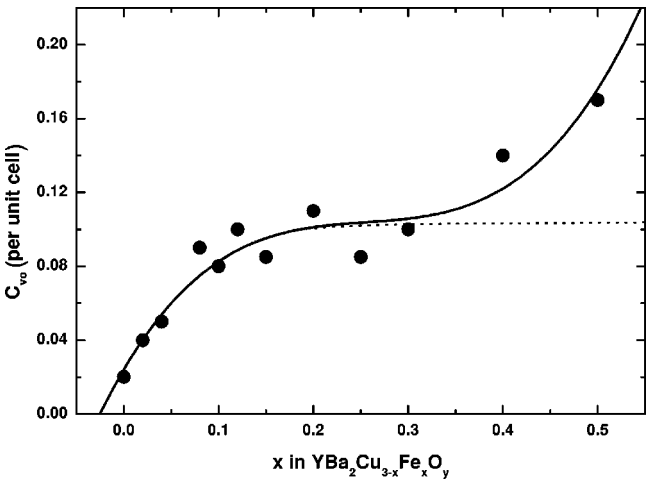

FIG. 6. Schematic drawing of C_{vo} vs x in the $YBa_2Cu_{3-x}Fe_xO_y$ system, which was drawn according to the data listed in Table I.

are trivalent. One additional oxygen is needed for every two substituted Fe atoms in the lattice in order to maintain the charge balance. Therefore, the ideal oxygen content can be expressed as

$$\text{ideal oxygen content} = 7 + 0.5x. \tag{9}$$

The calculated results (i.e., y_{cal} are listed in Table I).

The actual oxygen contents measured by experiment are also given in Table I. It is clear that the actual oxygen contents are smaller than their respective ideal values. We attribute this phenomenon to our preparation conditions. A previous study shows,[22] for undoped $YBa_2Cu_3O_y$, that the oxygen content can approaches 7 so that each Cu(1) has 4 oxygen coordination. However, the Co and Fe-doped YBCO specimens cannot get enough oxygen contents in air because their equilibrium oxygen pressure is higher than that of the pure YBCO. Sydow *et al.* obtained much higher oxygen contents and T_c by treating specimens in high-pressure O_2 or in O_3. Our samples were prepared in air, so the ambient oxygen partial pressure is lower than the equilibrium oxygen pressure of the materials and the oxygen content is less than the ideal values. As a result, valid oxygen vacancies were produced around the Fe atoms and their concentration increases with the increase of the Fe doping level.

We calculated the number of valid oxygen vacancies per unit cell (defined as C_{vo}) by subtracting the actual oxygen contents from the ideal values. The curve of C_{vo} versus x is plotted in Fig. 6. With the increasing of the doping content, C_{vo} increases monotonously.

In addition to oxygen vacancy, another important trapping center in this system is twin (and tweed) boundary. As we discussed in Sec. III B, the twin (and tweed) boundary density increases monotonously up to $x=0.12$ in our samples. Due to the phase transition when x exceeds 0.12, the tweed structure disappears and the boundary density drops consequently (see Fig. 3). Approximately, the twin (and tweed) boundary density C_{vt} is proportional to x below $x=0.12$ and falls suddenly between $x=0.12$ and 0.15.

Now we discuss the variation of τ_1 as a function of x on the basis of Eqs. (6)–(8). Before the phase transition ($x \leqslant 0.12$), both densities of the oxygen vacancy and the twin (and tweed) boundary increase monotonously with x that made P_{vo} and P_{vt} increase so τ_1 increases fast. An abrupt disappearance of the tweed structure leads to the sudden drop of τ_1 from $x=0.12$ to $x=0.15$. After that, the main factor that influences τ_1 is only the valid oxygen vacancy. τ_1 increases again when x is between 0.15 and 0.20 because the oxygen vacancy density increases. However, τ_1 reaches a saturation when $x>0.2$, indicating that the actual oxygen vacancy density does not increase anymore. This can be considered as a clue for the formation of Fe clusters when x is large.

Below $x=0.20$, Fe atoms substituted primarily on the Cu(1) sites. For every two substituted Fe atoms, approximately one additional oxygen atom is needed to incorporated into the Cu(1)-O layer.[23] However, upon increasing the Fe concentration, more and more Fe atoms will substitute in Cu(2) sites. This kind of replacement will not introduce additional oxygen because the oxygen coordination number of Cu(2) is already 5. In addition, if the Fe content is large enough, some Fe atoms will get together to form clusters.[24,25] Two neighboring Fe atoms in the clusters share one oxygen atom. Therefore, the number of oxygen atoms required by the Fe coordination when $x>0.2$ will less than that when x is small. When $x>0.2$, no more valid oxygen vacancies are generated and C_v will be a constant (see the dotted line in Fig. 6). Consequently, τ_1 reaches a saturation. The clustering behavior is in line with previous neutron-diffraction and x-ray absorption studies that find evidence for defect clustering in doped samples. The atomistic simulation technique has also indicated a strong tendency towards cluster formation.[24]

In summary, τ_1 varies as a function of the doping level, predominantly due to the variation of imperfections such as the oxygen vacancy and the twin (and tweed) boundary.

The positron lifetime τ is defined as the inverse of the overlap integral between the positron density (ρ_+) and the electron density (ρ_-). τ_2 remains a large value when $x \leqslant 0.12$ and has a large drop where the phase transition occurs, illustrating that the volume of cavities becomes smaller after the *O-T* structure phase transition and the electron density increases.

IV. CONCLUSIONS

A series of samples $YBa_2Cu_{3-x}Fe_xO_y$ ($x=0.0-0.50$) was prepared in air by the standard solid state reaction method. The crystal structure analysis reveals that $YBa_2Cu_{3-x}Fe_xO_y$ undergoes a structure phase transition from orthorhombic to tetragonal around $x=0.15$. Accompanied by the *O-T* phase transition, the tweed microstructure disappears and the positron short-lifetime component τ_1 falls abruptly. Therefore, the positron is very sensitive to the phase transition, which cannot be determined precisely by x-ray diffraction because it is troublesome to resolve the tiny orthorhombic distortion near the *O-T* phase transition. In order to give a reasonable explanation to our experimental results, we determined the

oxygen content and calculated the number of valid oxygen vacancies for each specimen. An empirical model is proposed to describe the relationship between the positron short-lifetime component τ_1 and the concentrations of imperfections. Considering the imperfections that can influence the lifetime of the positron, most researchers focused their attention on the oxygen vacancy. However, the twin and tweed boundaries are also indispensable trapping centers for positron annihilation. For specimens with $x \geqslant 0.20$, the doped Fe atoms and incoming oxygen tend to associate into clusters rather than being randomly distributed over the crystal lattice.

ACKNOWLEDGMENTS

This work is supported by the Ministry of Science and Technology of China (NKBRSF-G 19990646), the National Foundation of Natural Science of China (No. 19874017), the National Center for Research and Development on Superconductivity of China (No. J-A-5227) and the Province Foundation of Natural Science of Henan (No. 964020200).

*Electronic address: chengdon@aphy.iphy.ac.cn

[1] J. M. Tarascon *et al.*, Phys. Rev. B **37**, 7458 (1988).
[2] V. N. Narozhnyi and V. N. Kochetkov, Phys. Rev. B **53**, 5856 (1996).
[3] K. Westerholt, H. J. Wuller, H. Bach, and P. Stauche, Phys. Rev. B **39**, 11 680 (1989).
[4] V. E. Gasumyants, S. A. Kasmin, V. I. Kaidanov, and E. V. Vladimirskaya, Supercond., Phys. Chem. Technol. **5**, 674 (1992).
[5] Y. Xu, M. Suenaga, J. Tafto, R. L. Sabatin, and A. R. Moodenbaugh, Phys. Rev. B **39**, 6667 (1989).
[6] Z. Risto and M. Nieminen, J. Phys. Chem. Solids **52**, 1577 (1991).
[7] J. Zhang *et al.*, Phys. Lett. A **236**, 452 (1999).
[8] J. Zhang, S. Cao, F. Liu, and J. Lui, Phys. Rev. B **48**, 16 830 (1993).
[9] E. C. VonStetten *et al.*, Phys. Rev. Lett. **60**, 2198 (1988).
[10] Y. C. Jean *et al.*, Phys. Rev. Lett. **64**, 1593 (1990).
[11] B. Chakraborty, Phys. Rev. B **39**, 215 (1989).
[12] H. Zhang, Phys. Status Solidi A **121**, k207 (1990).
[13] S. Ishibashi, K. Suenaga, R. Yamamoto, M. Doyama, and T. Matsumoto, J. Phys.: Condens. Matter **2**, 3691 (1990).
[14] C. Dong, J. Appl. Crystallogr. **32**, 838 (1999).
[15] Z. Hiroi, M. Takano, Y. Takeda, R. Kanno, and Y. Bando, Jpn. J. Appl. Phys., Part 2 **27**, L580 (1988).
[16] L. C. Smedskjaer, B. W. Veal, D. G. Legnini, A. P. Paulikas, and L. J. Nowicki, Phys. Rev. B **37**, 2330 (1988).
[17] A. G. Balogy, W. Puff, L. Liszkay, and B. Mornal, Phys. Rev. B **38**, 2883 (1988).
[18] W. Brandt, *Positron Annihilation* (Academic, New York, 1967), p. 155.
[19] P. Hautojarvi, *Positrons in Solid*, Chinese edition (Science Publishing House, Beijing, 1983), p. 255.
[20] M. J. Puska and R. M. Nieminen, Rev. Mod. Phys. **66**, 841 (1994).
[21] A. Seeger, J. Phys. F: Met. Phys. **3**, 248 (1973).
[22] J. P. Sydow, R. A. Buhrman, and B. H. Moeckly, Appl. Phys. Lett. **72**, 3512 (1998).
[23] Y. Xu *et al.*, Phys. Rev. B **39**, 6667 (1989).
[24] M. S. Islam and C. Ananthamohan, Phys. Rev. B **44**, 9492 (1991).
[25] S. Katsuyama, Y. Ueda, and K. Kosuge, Physica C **165**, 405 (1989).